ADVANCES IN ATMOSPHERIC SCIENCES, VOL. 29, NO. 4, 2012, 769–781

Analysis of the Role Played by Circulation in the Persistent Precipitation over South China in June 2010

YUAN Fang[1,2] (远 芳), CHEN Wen*[1] (陈 文), and ZHOU Wen[3] (周 文)

[1] *Center for Monsoon System Research, Institute of Atmospheric Physics, Chinese Academy of Sciences, Beijing* 100190

[2] *Graduate University of the Chinese Academy of Sciences, Beijing* 100049

[3] *Guy Carpenter Asia-Pacific Climate Impact Center, School of Energy and Environment, City University of Hong Kong, Hong Kong*

(Received 17 January 2012; revised 3 February 2012)

ABSTRACT

South China (SC) experienced persistent heavy rain in June 2010. The climatic anomalies and related mechanism are analyzed in this study. Results show that the large-scale circulation pattern favorable for precipitation was maintained. In the upper level, the South Asian High and westerly jet stream provided a divergent circulation over SC. In the middle and low levels, an anomalous strong subtropical high (STH) extended to the South China Sea. The southwesterly monsoon flow along the northwest flank of the STH transported abundant water vapor from the western North Pacific, the Bay of Bengal, and the South China Sea to SC. The precipitation can be classified into two types: the West Siberia low (WSL)-induced low-level cyclone mode, and the STH-induced low-level jet mode. STH and WSL indices are defined to estimate the influence of these two systems, respectively. Analysis shows that both are critical for precipitation, but their respective contributions differ from year to year. In 2010, both were important factors for the heavy rainfall in June.

Key words: South China, precipitation, circulation, the subtropical high, the west Siberia low

Citation: Yuan, F., W. Chen, and W. Zhou, 2012: Analysis of the role played by circulation in the persistent precipitation over South China in June 2010. *Adv. Atmos. Sci.*, **29**(4), 769–781, doi: 10.1007/s00376-012-2018-7.

1. Introduction

Climatically, the summer monsoon breaks out in the fourth pentad of May in the South China Sea (SCS) (Murakami and Matsumoto, 1994; Lau and Yang, 1997; Wu and Wang, 2000; Zhou et al., 2005), and then jumps northward in middle or late June. After the onset of SCS summer monsoon (SCSSM), precipitation in South China (SC) increases dramatically, signifying the beginning of the monsoon season in this region, which is considered as the first step of the seasonal march of the monsoon rain belt (Ding and Chan, 2005). The most prominent feature of precipitation in SC is its double peak: the first peak (also called the first rainy season) from April to June is connected with fronts and the East Asian summer monsoon, and the second peak (the second rainy season) from July to October is mainly caused by cyclonic systems from the tropics (Tao, 1985). Previous studies have typically taken the total rainfall from June to August to represent summer precipitation (Huang and Sun, 1992; Chen et al., 2000). This is obviously inappropriate for SC. On the other hand, accompanying the onset of the East Asian summer monsoon, the properties of rainfall change dramatically (Yuan et al., 2010). Therefore, it would be more suitable to discuss the rainfall of June separately. Additionally, we calculated the monthly precipitation for 30 years (1981–2010) and found that among all the months, both precipitation and its variance are largest in June.

*Corresponding author: CHEN Wen, cw@post.iap.ac.cn

Many studies suggest that precipitation over SC is greatly influenced by the subtropical high (STH) over the Western North Pacific (WNP), as there will be more precipitation if the STH is stronger and lies west of its climatic state (Chang et al., 2000a; Yang and Sun, 2005; Bao, 2007; Zhou et al., 2009). By affecting the position and strength of the STH, many factors influence precipitation over East Asia. For example: SST and convective activities of the western Pacific warm pool (Huang and Sun, 1992); Pacific Decadal Oscillation (PDO) (Wang et al., 2008); South China Sea (SCS) SST and ENSO (Zhou et al., 2006; Zhou and Chan, 2007; Feng et al., 2010; Zhou et al., 2010); tropical oscillations (Zhou and Chan, 2005), large-scale equatorial heating anomalies (Wu et al., 2003); and Indian Ocean SST (Yuan et al., 2008; Xie et al., 2009; Huang et al., 2010; Wu et al., 2010).

Systems from middle and high latitudes can also affect precipitation over East Asia. For example, Zhang and Tao (1998) argued that the persistent blocking high over the Sea of Okhotsk could induce more precipitation in summer over East Asia. Tong et al. (2009) and Chang and Chen (1995) pointed out that the arrival of mid-latitude fronts may contribute to the onset of the SCSSM. Chan et al. (2000) pointed out that the equatorward-moving middle and high latitude fronts could release convective available potential energy and trigger deep convection over the SCS. The Ural blocking (Wang et al., 2010) and East Asian troughs (Wang et al., 2009) can also influence precipitation over East and Southeast Asia. Overall, the higher-latitude systems have received much less attention.

Mesoscale systems are known to be crucial for rainfall. Although large-scale circulation could provide a favorable background, mesoscale systems are the ones that directly bring rainfall (Tao, 1985). Both observational studies and numerical simulations have shown that precipitation usually happens on the right-hand side of the low-level cyclones (LLCs, also referred as southwest vortices) (Kuo et al., 1988; Chang et al., 2000b) and on the left-hand side of low-level jets (LLJs) (Chen and Yu, 1988; Chen et al., 1998).

The National Climate Centre (NCC) of China made forecasts for June 2010 (http://cmdp.ncc.cma.gov.cn/pred/md.php): slightly more precipitation in western SC and slightly less precipitation in eastern SC. However, what turned to be the case was a series of rain storms that attacked the whole region of SC. Heavy rainfall caused landslides, burst dams and traffic gridlocks, leading to hundreds of casualties, thousands of people becoming homeless and a direct economic loss of up to RMB 20 billion. Why this happened has yet to be addressed, and the aim of this paper is to find out the reasons.

The datasets and methodology are described in section 2. Some details about the persistent heavy rain event under study are given in section 3. Sections 4 and 5 present details of the large-scale circulations to explain the possible factors causing the extreme precipitation. And finally, section 6 outlines the conclusions.

2. Datasets and methodology

Daily and monthly mean NCEP/NCAR reanalysis data with a resolution of 2.5° by 2.5° (Kalnay et al., 1996) and daily rainfall data from 752 stations in China provided by the National Meteorological Information Centre for the period 1981–2010 were used in this study. The area of (20°–28°N, 105°–120°E), which includes 97 stations, was chosen to represent the region of SC. Data from 1981–2010 were used for calculating the climatic state. The typhoon data were obtained from the Joint Typhoon Warning Center.

The SCSSM onset date was defined as the day when the area-average of 850-hPa zonal winds over the SCS (110°–120°E, 5°–15°N) changes from negative to positive and remains positive for more than 6 days (Wang et al., 2004; Mao and Chan, 2005; Zhou et al., 2005). Based on this, the onset date in 2010 was established as 22 May. With the interval of 2.5°, there are nine lines of longitude between 105°E and 125°E, and the meridional location of the STH ridge (i.e. its latitude) was defined as the mean value of the latitudes of the maximum 500-hPa geopotential height on every line of longitude (Peng and Sun, 2002).

3. Description of the persistent heavy rain in June 2010

SC experienced a large amount of precipitation and suffered severe floods in June 2010. During this month, a total of 203 rainstorms (precipitation over 50.0 mm in 24 h) were recorded at 97 stations in South China, which was almost double the climatological mean value. In fact, the June of 2010 was the third wettest in the last 30 years. Figure 1 shows the distribution of the precipitation with its climatology and anomalies. It is clear that most of the rainfall (Fig. 1a) and also the positive rainfall anomaly (Fig. 1c) were located south of the Yangtze River. Half of the SC region had 60% more precipitation (Fig. 1d) than its climatic state (Fig. 1b). Most other places in China, however, experienced much dryer conditions during this month, except for the northern part of Qinghai Province (Fig. 1d).

The persistent precipitation over SC lasted for the whole month apart from a short dry period around 4 June (Fig. 2a). At the end of the month, the STH jumped northward (Fig. 2b), signifying the end

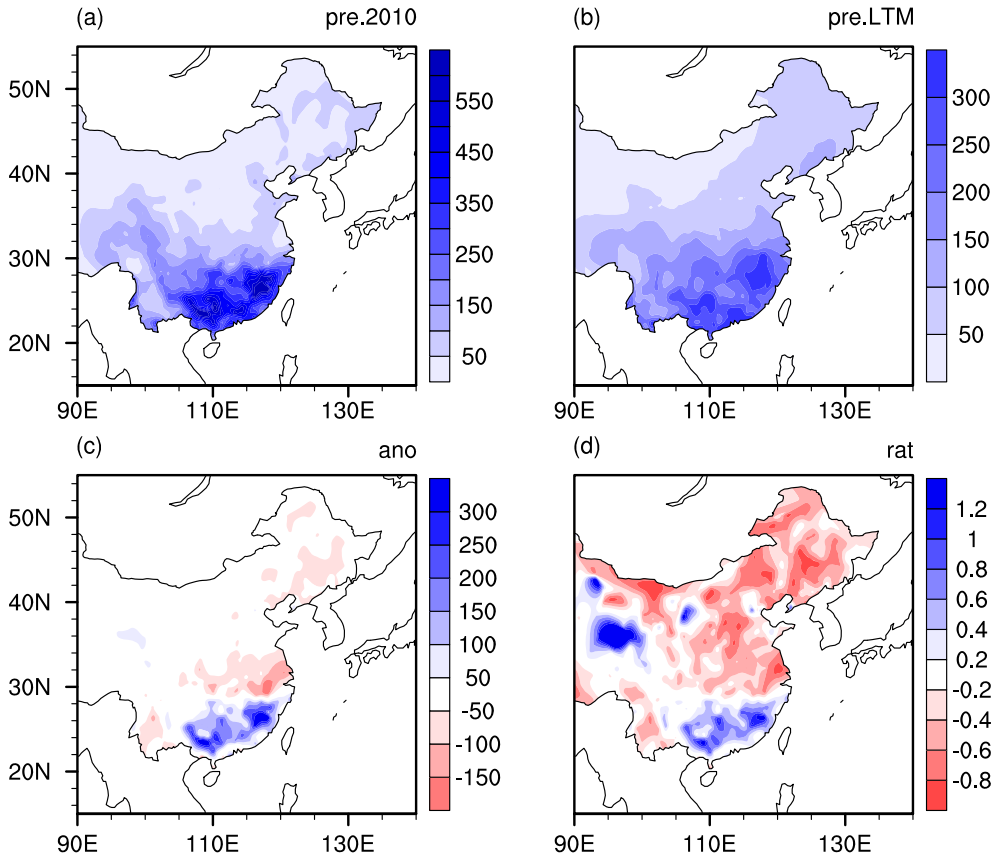

Fig. 1. Precipitation of (a) June 2010 (mm), (b) long-term mean condition (1981–2010, mm), (c) precipitation anomaly of 2010, and (d) precipitation anomaly percentage of 2010.

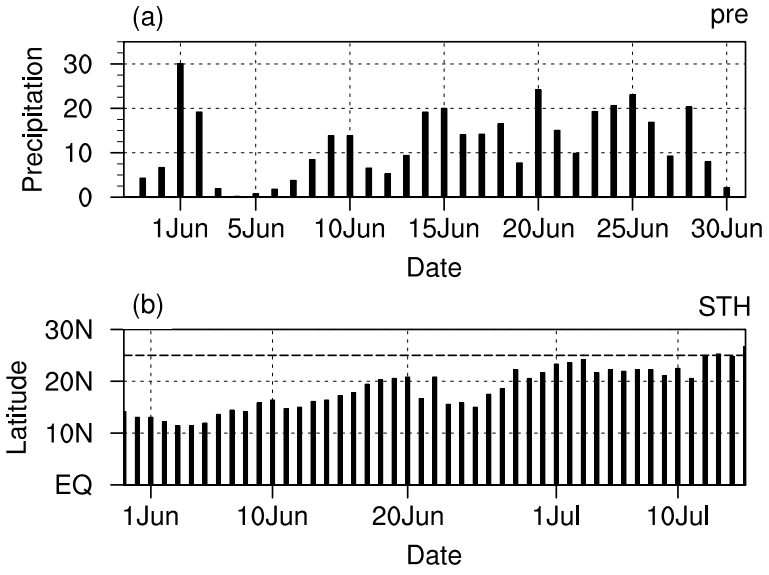

Fig. 2. (a) Area mean daily precipitation of SC (mm) and (b) meridional location of subtropical high ridge over (105°–125°E).

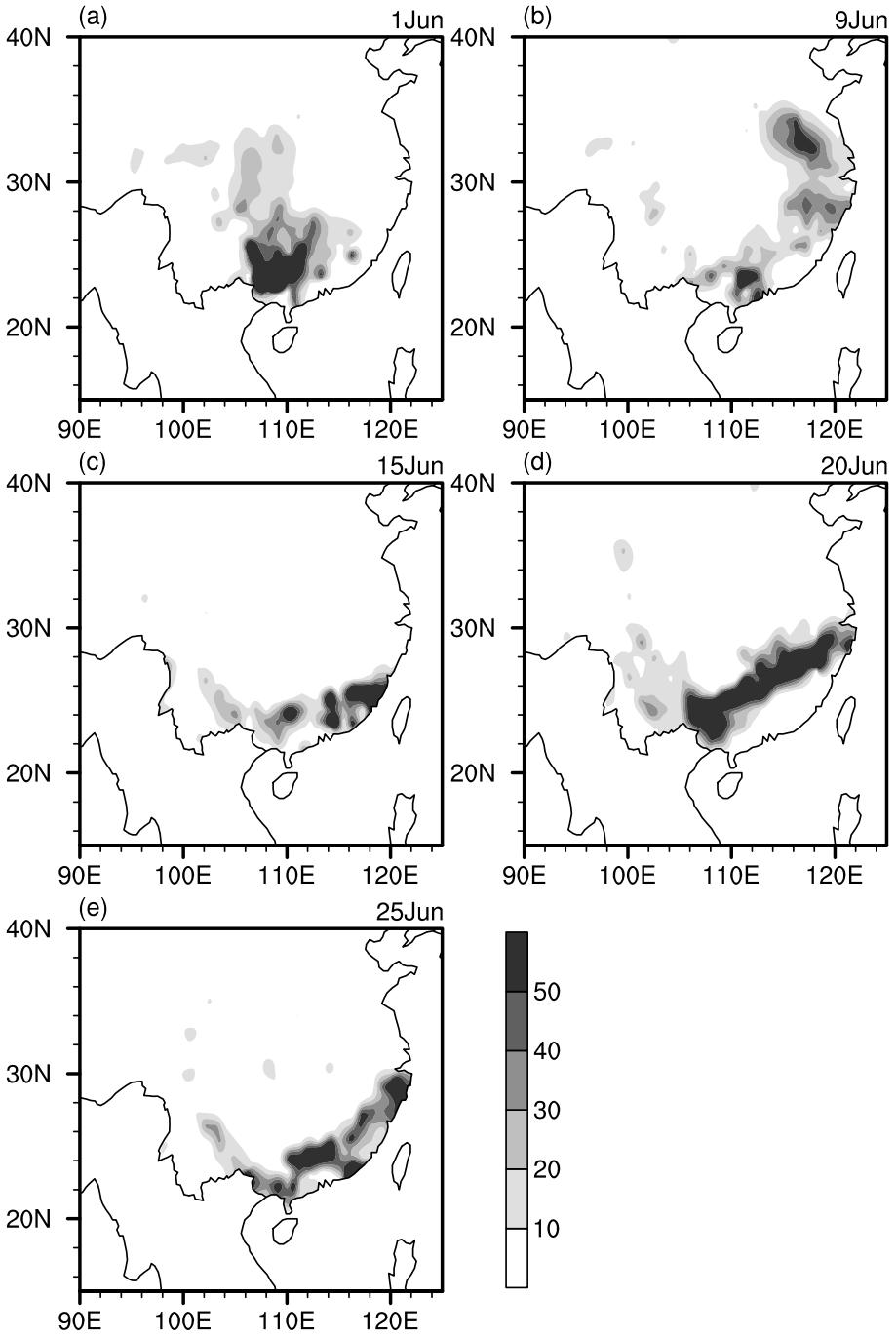

Fig. 3. Daily distribution of precipitation (mm).

of monsoon precipitation in SC. We analyzed the daily distributions of circulation and rainfall and found that the whole period can be generally divided into five processes (i.e. cases). Since these processes occurred one after another, temporally it is difficult to separate them exactly. Here, we denote each process by its rainfall peak day, which were: 1 June, 9 June, 15 June, 20 June and 25 June (Fig. 3). For convenience, in the following paragraphs of this section the height and wind fields are all limited to the 850 hPa level, and most of the figures mentioned below are not shown.

On 30 May, there were convergent winds to the east of the Tibetan Plateau (TP) and these winds developed into a cyclone on 1 June (Fig. 4a) during the southeastward propagation, and moved away from mainland China on 3 June. The second process was

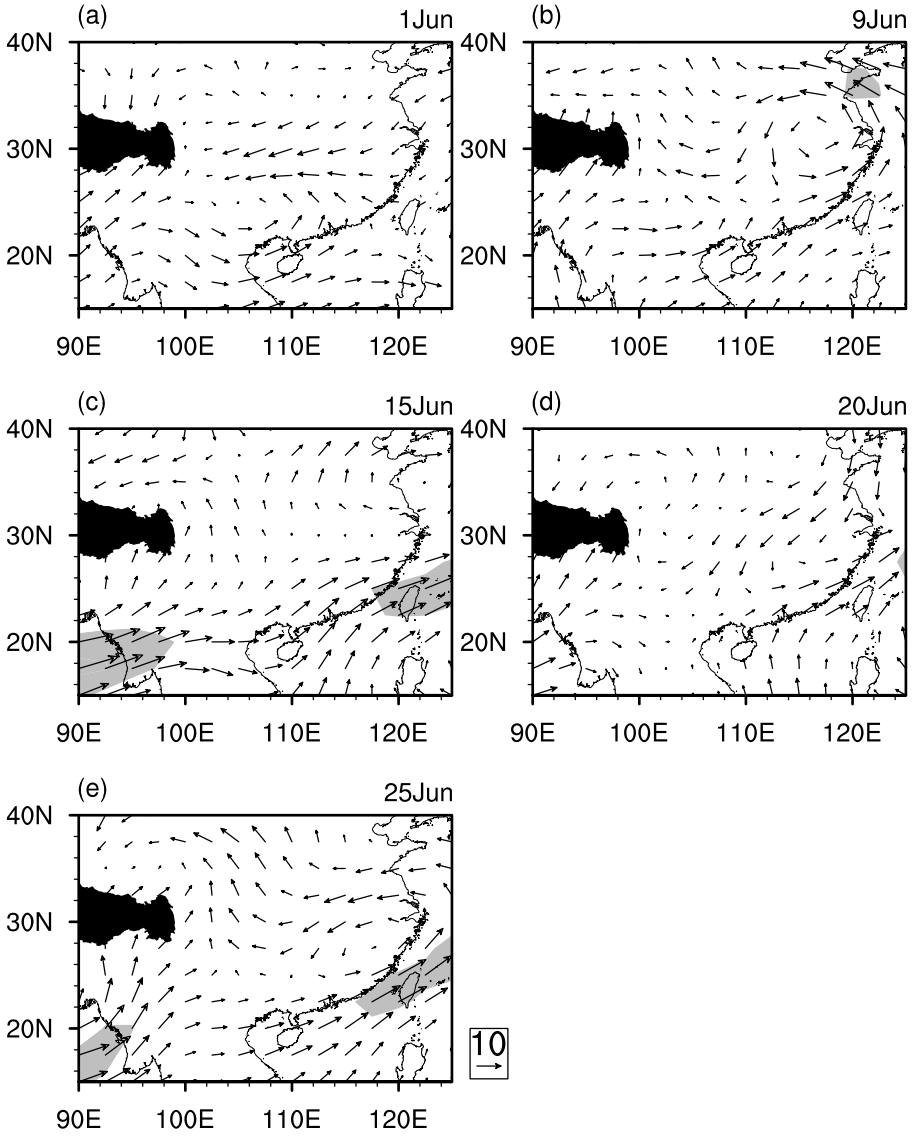

Fig. 4. Daily distribution of 850 hPa wind (vectors, m s^{-1}) and shadings denotes the area with wind speed over 12 m s^{-1}.

quite similar to the first. Convergence also showed up near the northeast flank of the TP on 5 June and developed during its eastward propagation. A clear cyclone can be seen in the wind field on 8 and 9 June (Fig. 4b) and this cyclone moved to the East China Sea on 10 June.

For the third process, which took place from 13 to 16 June, there was no cyclone, but a strong LLJ can be observed (Fig. 4c); strong rainfall was located on the left side of the LLJ (Fig. 3d) where the circulation was favorable for precipitation because of the cyclonic wind shear (Chen and Yu, 1988; Chen et al., 1998). It is interesting to note that from 13 to 20 June the STH ridge was located between 16°–20°N and in the corresponding wind field a strong LLJ was found in the southwesterly wind, indicating a direct connection between STH and precipitation.

The fourth process was accompanied by a cyclone, but was more complex than the first two. On 17 and 18 June, there was a strong low pressure near (40°N, 110°–120°E) stretching down to 28°N and consequently a wind shear near the mid-lower reaches of the Yangtze River was produced by the northerly wind and southerly LLJ; at the same time, the convergent circulation appeared near the east of the TP and a cyclone developed on 19 June. This cyclone was linked together with the wind shear generated on 17 June. On 20 June, this cyclonic-wind shear system evolved

into a horizontal trough (Fig. 4d) and then moved eastward to the East China Sea the next day (21 June). For the fifth process, a wind shear showed up along the mid-lower reaches of the Yangtze River on 23 June, developed into a cyclone (Fig. 4e) and then moved to the East China Sea on 26 June.

Additionally, new convergence near to the east of the TP showed up from 25 June and brought about a large amount of precipitation for SC, but because it occurred around the end of June, the ridge of the subtropical high (STH) jumped northward by about 8° from 16° to 24°N (Fig. 2b) and the SC region was covered by the STH. Thus, in the wind field the convergent circulation did not develop into a cyclone and in this study we do not cover this "short-lived" process.

4. Circulations associated with the precipitation event

4.1 *Favorable background circulations and water vapor transport*

At the 200 hPa level, the South Asia High (SAH) covered the whole of the southern part of Asia (Fig. 5a) and served as the centre of the divergence field (Fig. 6a). In the mid-latitudes, there was a blocking high located between the Lake of Baikal and the Sea of Okhotsk, and under its influence the axis of the westerly jet moved southward (Fig. 5b), which is favorable for precipitation over the southern part of China (Liang and Wang, 1998; Lu, 2004; Lin and Lu, 2005).

In the 500-hPa geopotential height field (Fig. 5c), compared with the climatic state, the STH, which is denoted by the 5880-gpm contour, was much stronger in the west north Pacific (WNP) and extended westward to the SCS area. As a consequence, water vapor could be transported along the northwest edge of the STH to SC (Fig. 7). From Fig. 7a we can see that there were two branches of water vapor transported to SC: one was from the west, the Bay of Bengal and the Arabian Sea; and the other from the east, the WNP, along the northwest edge of the STH to SC.

Not only the zonal, but also the meridional location of the STH was important for where precipitation occurred. The vertically-integrated water vapor flux (Fig. 7b) shows that, in the region of SC, there was weak equatorward transport of water vapor during the dry period around 4 June, and strong northeastward transport during the wet periods. Comparing Figs. 7b and 2b it can be seen that the water vapour flux corresponds well with the variation of the STH ridge. During the dry period around 4 June, the STH ridge was at its lowest latitude, indicating that northeastward water vapor transport was at its weakest. On the other hand, at the end of June, the STH jumped northward to 25°N and a correspondingly large amount of water vapor was transported to the mid-lower reaches of the Yangtze River.

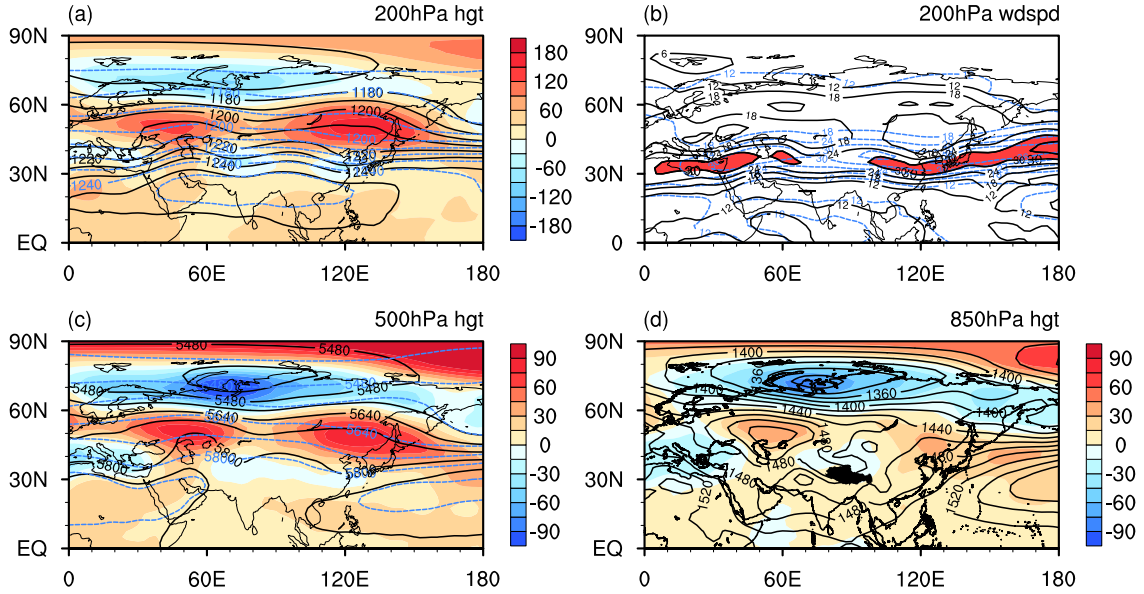

Fig. 5. Geopotential height (solid contour) of June 2010 and its anomaly (shadings) and long term mean condition (dashed contour) of (a) 200 hPa (10 gpm), (c) 500 hPa (gpm) and (d) 850 hPa (gpm) and (b) 200 hPa wind speed (m s^{-1}, solid contour, shadings denote the area larger than 30 m s^{-1}) of June 2010 and long term mean condition (m s^{-1}, dashed contour).

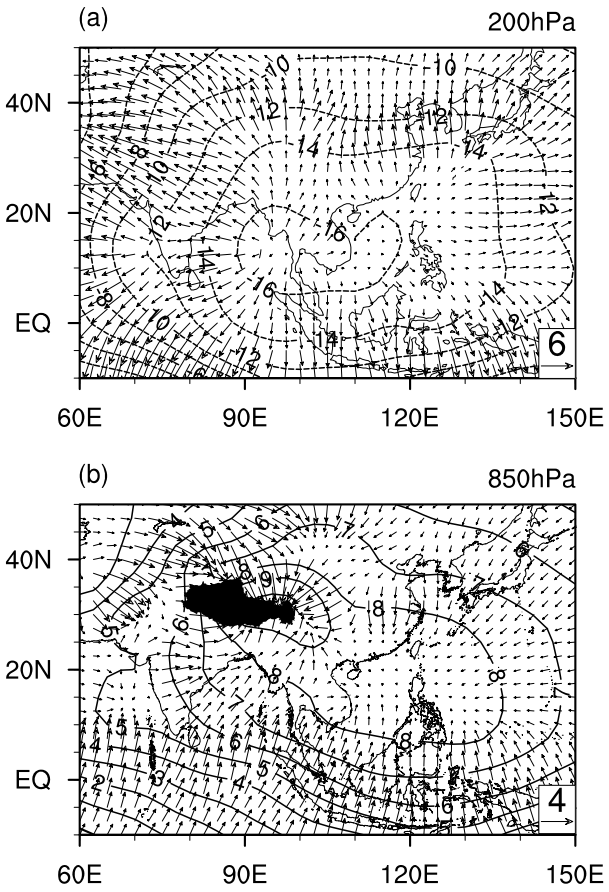

Fig. 6. Divergent wind (vectors, m s^{-1}) and velocity potential (contour, 10^7 m^2 s^{-1}) of June 2010, (a) 200 hPa and (b) 850 hPa.

Additionally, the forecast for the 500-hPa geopotential height field made at the time by the NCC of China (http://cmdp.ncc.cma.gov.cn/pred/md.php) reveals that, in June 2010, the 5880-gpm contour was expected to be located along the middle and lower reaches of the Yangtze River, much farther north compared to the what was subsequently observed. Furthermore, the east part of SC was expected to be controlled by the STH, which was not conducive to the occurrence of precipitation. Consequently, the percentage figure for the ensemble mean precipitation anomaly for June shows a positive anomaly over western SC and a negative anomaly over eastern SC, whereas in Fig. 2c a positive anomaly can be seen over the whole of SC.

In the 850-hPa geopotential height field (Fig. 5d), there was a negative anomaly to the south of the TP, serving as the centre of low-level convergence (Fig. 6b), and the corresponding area in the precipitation field had 60% more rainfall than the climatic condition (Fig. 1d). SC was under the influence of convergence.

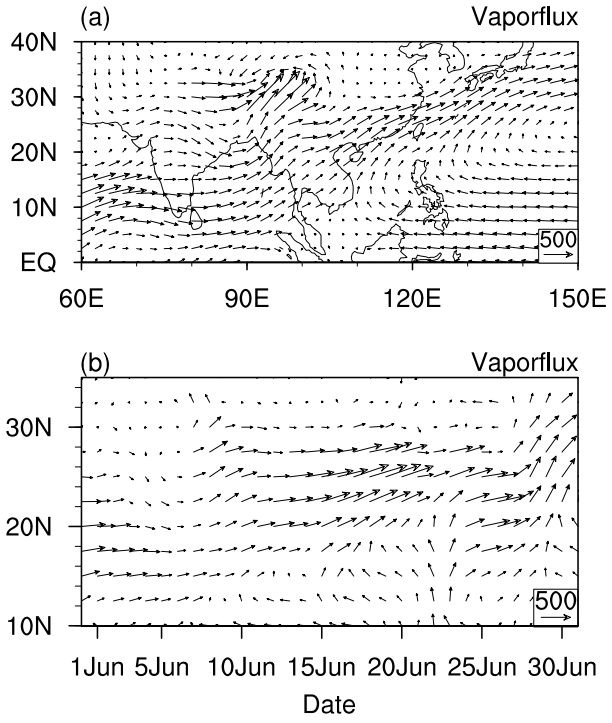

Fig. 7. (a) Vertically integrated water vapour flux (kg m^{-1} s^{-1}) of June 2010, and (b) averaged vertically integrated water vapour flux (kg m^{-1} s^{-1}) over (105°–120°E).

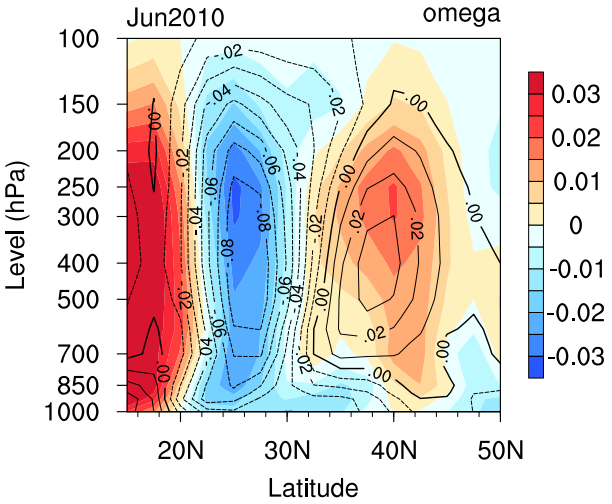

Fig. 8. Latitude-height section (along 105°–120°E) of omega (Pa s^{-1}) and its anomaly (shadings).

The warm and wet monsoon flow converged with cold air from the north, bringing large amounts of precipitation to SC.

Figure 8 shows the latitude–height section of vertical velocity (ω) and indicates that SC experienced

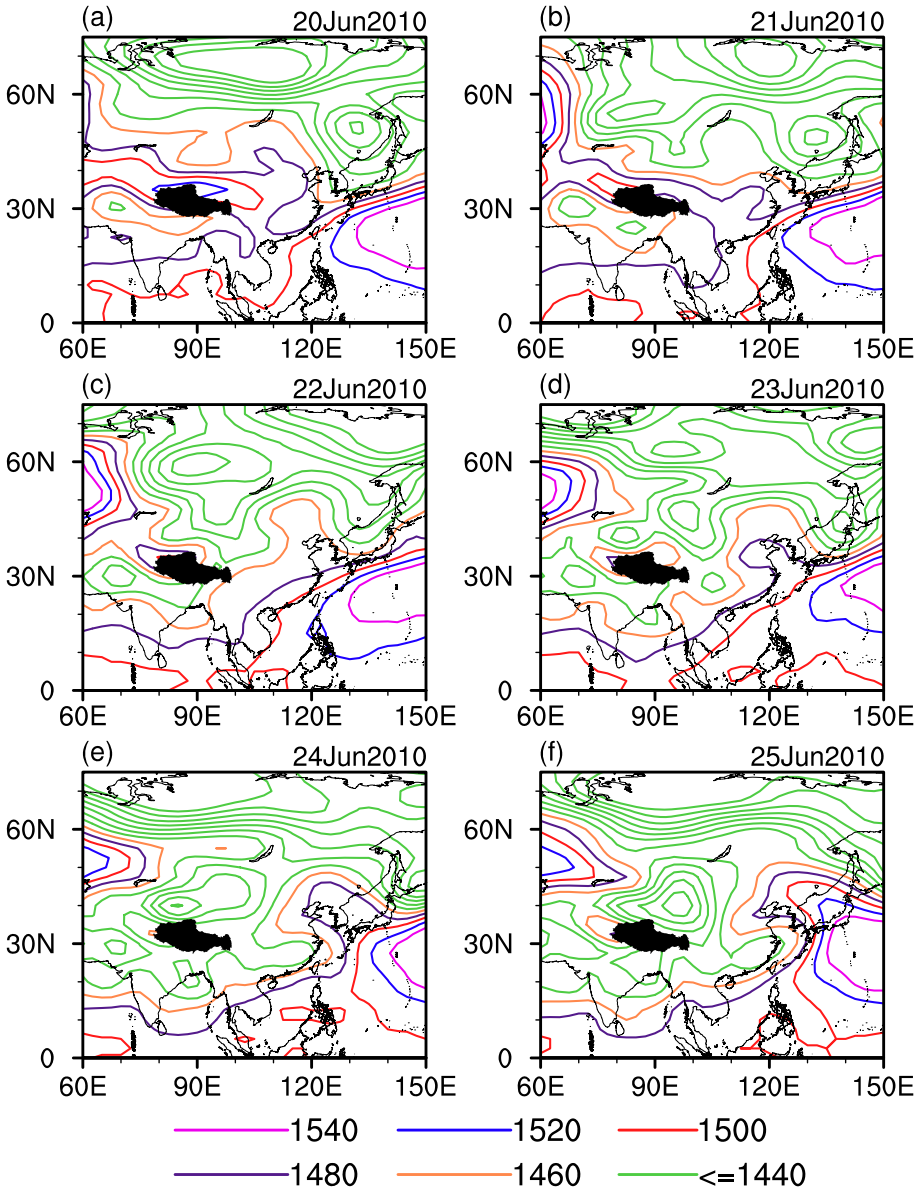

Fig. 9. Daily distribution of 850 hPa geopotential height (gpm, interval of the green contour: 20 gpm).

anomalous strong upward motion in June 2010. This was the combined result of multiple systems, including the anomalous ridge and southward displacement of the mid-latitude westerly jet and anomalous strong SAH and STH. Note that there was anomalous downward motion in middle latitudes and tropics.

4.2 *Influence of systems from higher latitudes*

Most previous studies on summer precipitation in SC have focused on the influence of tropical systems, with much less attention having been given to those systems from the mid-high latitudes. Nevertheless, obvious circulation anomalies are noticeable in higher latitudes. In particular, with the present event, an anomalous low was apparent over western Siberia, as seen in Figs. 5a, c and d. Thus, a natural question is whether this anomalous low could have influenced precipitation in SC, and how?

As mentioned in section 3, for four of the five cases (1 June, 9 June, 20 June and 25 June) the occurrence and movements of precipitation were accompanied by LLCs (Figs. 4a, b, d and e), which developed from convergent circulations near the east of the TP. We further found that these convergent circulations were usually preceded by strong low pressure propagating from higher latitudes in the height field. We take the fifth case as an example to show the detailed variation.

Figure 9 shows that on 20 June the area with a

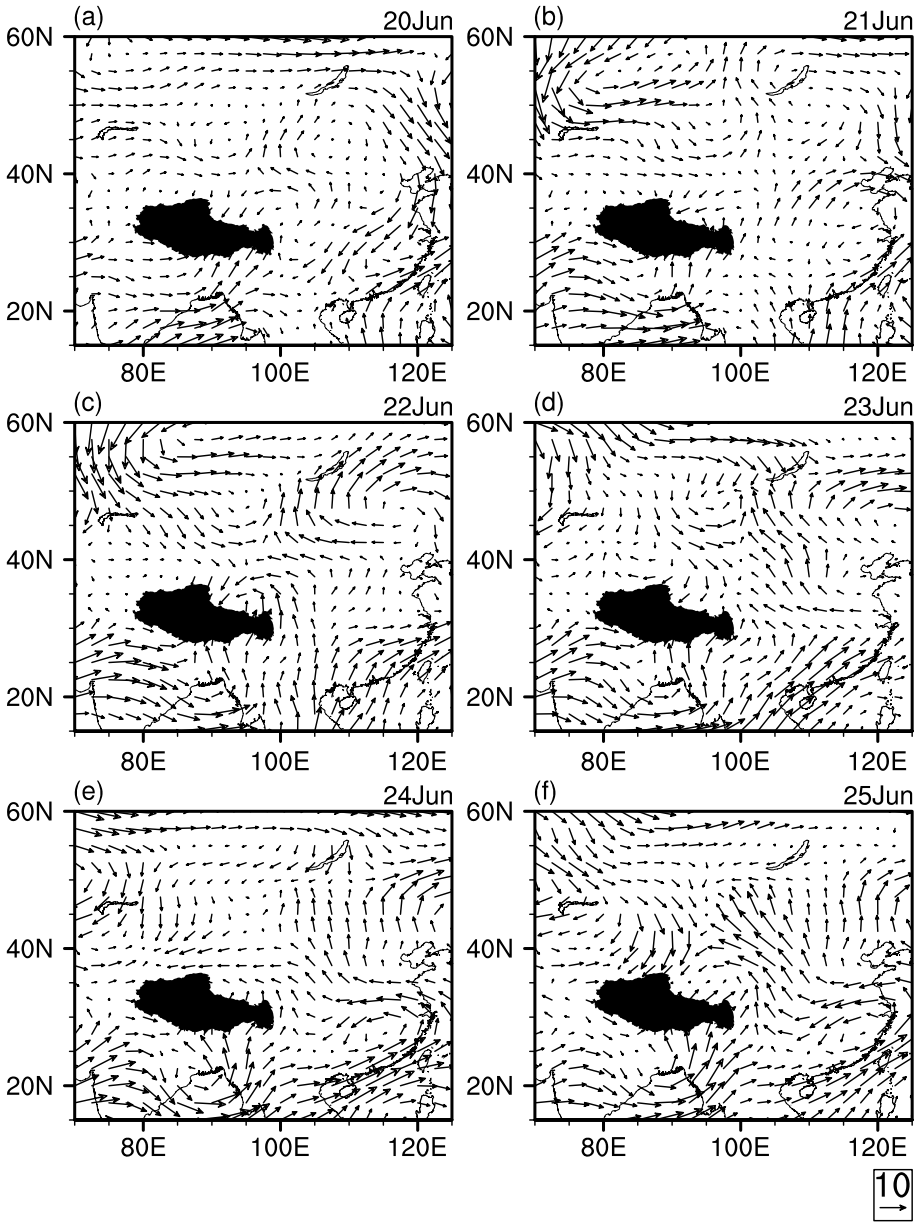

Fig. 10. Daily distribution of 850 hPa wind (m s^{-1}).

geopotential height lower than 1460 gpm (the orange contour) was first confined to the north of 50°N, and then stretched southward almost 10° per day before, on 25 June, the 1460 gpm-contour covered the whole of the continent. Figure 10 shows the corresponding 850-hPa wind field. As can be seen, on 20 and 21 June the winds in the mid-latitudes were somewhat disorganized (Figs. 10a and b). Distinct convergent circulation near the northeast flank of the TP (Fig. 10c) can be observed when the trough extended to 35°N on 22 June (Fig. 9c). With the further intrusion of low pressure, a wind shear showed up over SC on 23 June (Fig. 10d) and then developed into a cyclone (Fig. 10e) and moved eastward to the East China Sea on 25 June (Fig. 10f).

Three of the other cases were similar in their detail to the fifth, described above. However, one case (15 June) was not accompanied by LLC, but by a LLJ (Fig. 4c), which was associated with the STH, as mentioned in section 3. The low pressure from high latitudes seems to not be as important as in the other cases, but it still helped to increase the meridional geopotential height gradient, thereby strengthening the LLJ (Tong et al., 2009).

To summarize sections 3 and 4, we found that the West Siberia low (WSL) likely plays an important role in precipitation in the lower latitudes. When low pressure from high latitudes near West Siberia prop-

agates to the mid-latitudes (about 30°–40°N) it will start a convergent circulation and, with a favorable background circulation, this convergence can develop into a strong cyclone (i.e. LLC) during its southward propagation, bringing about large amounts of precipitation. The STH is also very important for this precipitation. It determines the extent of large-scale water vapor transport and, moreover, it has a direct impact upon precipitation associated with the LLJ.

We also analyzed the occurrence of precipitation during the period 1981–2009 and found that in June over SC it can generally be divided into two types: the WSL-induced LLC mode and the STH-induced LLJ mode. It should be emphasized that the LLJs mentioned here are limited to those that are generated due to the enhancement of southwesterly winds on the northwest flank of the STH, not because of strong cyclones.

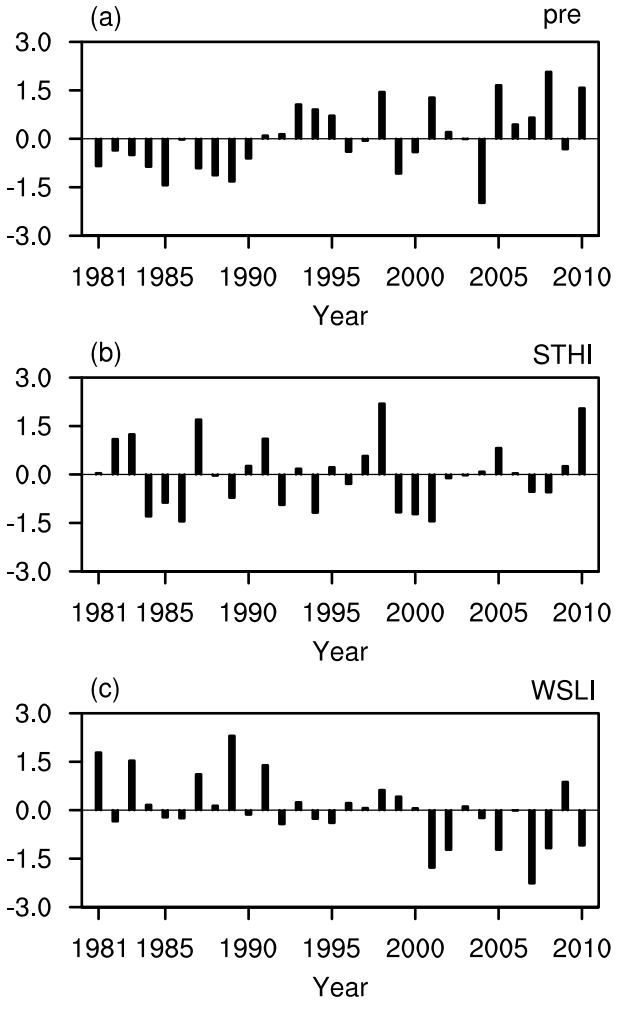

Fig. 11. Time series of normalized (a) area mean precipitation of June over SC, (b) Subtropical High Index, and (c) West Siberia Low Index.

5. Discussion about the influence of the STH and WSL

Among all the factors, the anomalies of the STH and WSL were likely to have been the main influences. Figure 11a presents the time series of precipitation for June over the past 30 years. From its correlations with 500-hPa geopotential height and sea level pressure (SLP; Fig. 12), it can be seen that there is a positive correlation region over the SCS and WNP (Fig. 12a) and significant negative correlation near West Siberia (Fig. 12b). This result is consistent with the above analysis. The composite differences of 500-hPa height and SLP fields of wet years (when precipitation was above a standard deviation of 0.5) and dry years (when precipitation was below a standard deviation of −0.5) show a similar pattern (figures not shown).

We defined the area-mean SLP in the region (55°–70°N, 60°–90°E) as the WSL index (I_{WSL}; Fig. 11b), and the area-mean 500-hPa geopotential height in the region (5°–20°N, 105°–160°E) as the Subtropical High index (I_{sth}; Fig. 11c). Figure 13 presents the regression of precipitation with respect to the normalized I_{sth}

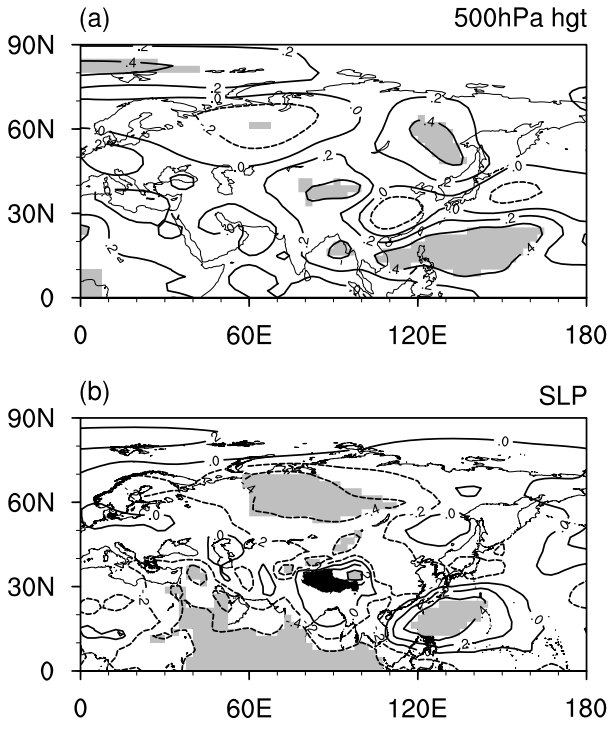

Fig. 12. Correlation of (a) 500 hPa geopotential height and (b) Sea Level Pressure of June with respect to normalized precipitation from 1981–2010. Shadings denote regions with correlation significant over the 0.05 level.

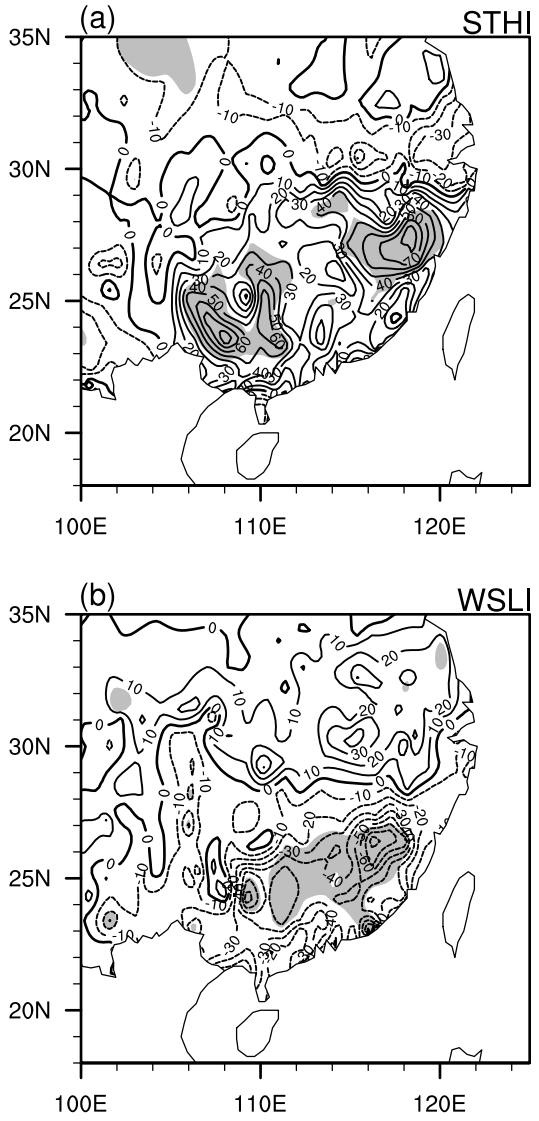

Fig. 13. Regression of precipitation of June with respect to (a) normalized subtropical high index and (b) West Siberia low index. Shadings denote regions with correlation significant over the 0.05 level.

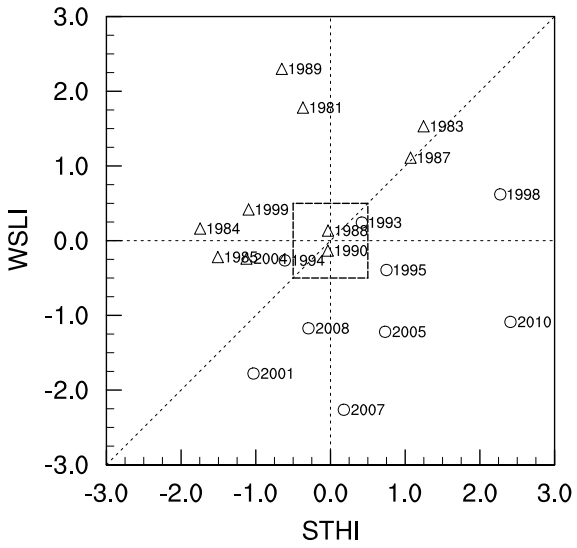

Fig. 14. Scatter plot of precipitation with the subtropical high index and West Siberia low index. Circles denote the wet years (the years when precipitation above 0.5 standard deviation in Fig. 11a) and triangles denote the dry years (the years when precipitation below −0.5 in Fig. 11a).

and I_{WSL}. As can be seen, in SC, precipitation has a significant positive correlation with I_{sth} and a negative correlation with I_{WSL}, which means that when the STH is over the SCS and WNP, or the WSL is stronger (e.g. higher I_{sth} or lower I_{WSL}), SC will experience more precipitation.

Figure 14 presents the relationship of these two indices with precipitation. It can be seen that all the wet years, except 1994, are located on the right-hand side of the diagonal, with I_{WSL} below 0.5 (except 1998) and I_{sth} above −0.5 (except 2001 and 1994). In contrast, except for 1990, all the dry years are located on the left-hand side of the diagonal, with I_{WSL} above −0.5 and I_{sth} below 0.0 (except 1983 and 1987).

Based on Fig. 14, we did some preliminary analysis on other years besides 2010. For convenience, we won't present the figures mentioned below. Generally speaking, it was found that more LLJ-mode (LLC-mode) precipitation is likely to have occurred with a larger (smaller) I_{sth} (I_{WSL}). For example, the precipitation in 2007 is predicted to have been more linked with LLC-mode precipitation, while in 1998 more LLJ-mode precipitation showed up. At the same time, a lower I_{sth} points towards insufficient water vapor, such that in 1984, for example the STH in the SCS was probably very weak and more water vapor was thus transported to the SCS and western tropical Pacific, resulting in the whole of eastern China experiencing 40% less precipitation than usual. In addition, in 1983 and 1987, the STH was strong and westward, but the meridional position was slightly northward, meaning more water vapor would have been transported to the mid-lower reaches of the Yangtze River and North China, where more precipitation was subsequently observed.

Figures 13 and 14 indicate that both the STH and the WSL are critical for precipitation patterns in SC, but their respective contributions differ from year to year. In 2010, both were anomalously strong and thus extremely favorable for the heavy and persistent rainfall that occurred over SC in June of that year.

6. Conclusions

This study has provided an analysis of the precipitation that occurred in June 2010 in SC when a series of rain storms hit the region and caused a number of disastrous effects for the local population. Our results show that the background circulations were stable and favorable for the precipitation that was observed. At the upper level, the SAH and the westerly jet stream provided a divergent circulation for SC. In the 500-hPa geopotential height field, there was an anomalously strong STH over the SCS. The southwesterly monsoon winds along the northwest edge of the STH supplied abundant water vapor from the WNP, Bay of Bengal and Arabian Sea to SC. The longitudinal location of the STH was found to be critical since it determined whether water vapor could be transported to SC or the SCS, or the mid-lower reaches of the Yangtze River.

The whole period of precipitation in June 2010 can be described as having been comprised of five individual cases. Four of these five cases were associated with LLCs and one was caused by a LLJ. The LLCs developed from convergent circulations near the east of the TP and were later related with low pressure systems originated from the West Siberia region. The LLJ was related with the enhancement of southwesterly winds on the edge of the STH, which in fact reflected the variation of the STH. We also carried out some preliminary analysis of precipitation for the period 1981–2009 and found that it can be classified into two types: the West Siberia low (WSL)-induced LLC mode and the STH-induced LLJ mode.

STH and WSL indices were defined in order to estimate the influence of these two systems. Our analysis shows that both are critical for precipitation patterns, but their respective contributions differ from year to year. Also, generally speaking, there will be more LLJ-mode (LLC-mode) precipitation with a larger (smaller) $I_{\rm sth}$ ($I_{\rm WSL}$). In 2010, both were important factors for the heavy rainfall that occurred in June of that year.

Acknowledgements. Part of this study was carried out by F. Yuan as a visiting research assistant at the City University of Hong Kong. This work was supported by the National Basic Research Program of China (Grant No. 2009CB421405) and the National Natural Science Foundation of China (Grant Nos. 41025017 and 40921160379), partly supported by City University of Hong Kong (Grant No. 7002717).

REFERENCES

Bao, M., 2007: The statistical analysis of the persistent heavy rain in the last 50 years over China and their backgrounds on the large scale circulation. *Chinese J. Atmos. Sci.*, **31**, 779–792. (in Chinese)

Chan, J. C. L., Y. G. Wang, and J. J. Xu, 2000: Dynamic and thermodynamic characteristics associated with the onset of the 1998 South China Sea summer monsoon. *J. Meteor. Soc. Japan*, **78**, 367–380.

Chang, C. P., and G. T. J. Chen, 1995: Tropical circulations associated with southwest monsoon onset and westerly surges over the South China Sea. *Mon. Wea. Rev.*, **123**, 3254–3267.

Chang, C. P., Y. Zhang, and T. Li, 2000a: Interannual and interdecadal variations of the East Asian summer monsoon and tropical Pacific SSTs. Part I: Roles of the subtropical ridge. *J. Climate*, **13**, 4310–4325.

Chang, C. P., L. Yi , and G. T. J. Chen, 2000b: A numerical simulation of vortex development during the 1992 East Asian Summer Monsoon onset using the Navy's regional model. *Mon. Wea. Rev.*, **128**, 1604–1631.

Chen, C., W. K. Tao, P. L. Lin, G. S. Lai, S. Tseng, and T. C. C. Wang, 1998: The intensification of the low-level jet during the development of mesoscale convective systems on a mei-yu front. *Mon. Wea. Rev.*, **126**, 349–371.

Chen, G. T. J., and C. C. Yu, 1988: Study of low-level jet and extremely heavy rainfall over northern Taiwan in the Mei-Yu season. *Mon. Wea. Rev.*, **116**, 884–891.

Chen, W., H. F. Graf, and R. H. Huang, 2000: The interannual variability of East Asian winter monsoon and its relation to the summer monsoon. *Adv. Atmos. Sci.*, **17**, 48–60.

Ding, Y. H., and J. C. L. Chan, 2005: The East Asian summer monsoon: An overview. *Meteor. Atmos. Phys.*, **89**, 117–142.

Feng, J., W. Chen, C. Y. Tamc, and W. Zhou, 2010: Different impacts of El Niño and El Niño Modoki on China rainfall in the decaying phases. *Int. J. Climatol.*, **115**, doi: 10.1002/joc.2217.

Huang, G., K. M. Hu, and S. P. Xie, 2010: Strengthening of tropical Indian Ocean teleconnection to the Northwest Pacific since the mid-1970s: An atmospheric GCM study. *J. Climate*, **23**, 5294–5304.

Huang, R. H., and F. Y. Sun, 1992: Impacts of the tropical western Pacific on the East Asian summer monsoon. *J. Meteor. Soc. Japan*, **70**, 243–256.

Kalnay, E., and Coauthors, 1996: The NCEP/NCAR 40-year reanalysis project. *Bull. Amer. Meteor. Soc.*, **77**, 437–471.

Kuo, Y. H., L. S. Cheng, and J. W. Bao, 1988: Numerical simulation of the 1981 Sichuan flood. I: Evolution of a mesoscale southwest vortex. *Mon. Wea. Rev.*, **116**, 2481–2504.

Lau, K. M., and S. Yang, 1997: Climatology and interannual variability of the Southeast Asian summer monsoon. *Adv. Atmos. Sci.*, **14**, 141–162.

Liang, X. Z., and W. C. Wang, 1998: Associations between China monsoon rainfall and tropospheric jets. *Quart. J. Roy. Meteor. Soc.*, **124**, 2597–2623.

Lin, Z. D., and R. Y. Lu, 2005: Interannual meridional displacement of the East Asian upper-tropospheric

jet stream in summer. *Adv. Atmos. Sci.*, **22**, 199–211.

Lu, R. Y., 2004: Associations among the components of the East Asian summer monsoon system in the meridional direction. *J. Meteor. Soc. Japan*, **82**, 155–165.

Mao, J. Y., and J. C. L. Chan, 2005: Intraseasonal variability of the South China Sea summer monsoon. *J. Climate*, **18**, 2388–2402.

Murakami, T., and J. Matsumoto, 1994: Summer monsoon over the Asian continent and the western North Pacific. *J. Meteor. Soc. Japan*, **72**, 719–745.

Peng, J. Y., and Z. B. Sun, 2002: Influence of spring equatorial eastern Pacific SSTA on western Pacific subtropical high. *Journal of Nanjing Institute of Meteorology*, **23**, 191–195. (in Chinese)

Tao, S. Y., 1985: *Heavy Rains in China*. Science Press, 255pp.

Tong, H. W., J. C. L. Chan, and W. Zhou, 2009: The role of MJO and mid-latitude fronts in the South China Sea summer monsoon onset. *Climate Dyn.*, **33**, 827–841.

Wang, B., Y. Zhang, and M. M. Lu, 2004: Definition of South China Sea monsoon onset and commencement of the East Asia summer monsoon. *J. Climate*, **17**, 699–710.

Wang, L., W. Chen, W. Zhou, and R. H. Huang, 2009: Interannual variations of East Asian trough axis at 500 hPa and its association with the East Asian winter monsoon pathway. *J. Climate*, **22**, 600–614.

Wang, L., W. Chen, W. Zhou, J. C. L. Chan, D. Barriopedro, and R. H. Huang, 2010: Effect of the climate shift around mid 1970s on the relationship between wintertime Ural blocking circulation and East Asian climate. *Int. J. Climatol.*, **30**, 153–158.

Wu, R. G., and B. Wang, 2000: Interannual variability of summer monsoon onset over the western North Pacific and the underlying processes. *J. Climate*, **13**, 2483–2501.

Wu, R. G., Z. Z. Hu, and B. P. Kirtman, 2003: Evolution of ENSO-related rainfall anomalies in East Asia. *J. Climate*, **16**, 3742–3758.

Wu, R. G., Z. Wen, S. Yang, and Y. Li, 2010: An interdecadal change in southern China summer rainfall around 1992/93. *J. Climate*, **23**, 2389–2403.

Xie, S. P., J. Hafner, H. Tokinaga, Y. Du, T. Sampe, K. M. Hu, and G. Huang, 2009: Indian Ocean capacitor effect on Indo-western Pacific climate during the summer following El Nino. *J. Climate*, **22**, 730–747.

Yang, H., and S. Sun, 2005: The characteristics of longitudinal movement of the subtropical high in the western Pacific in the pre-rainy season in South China. *Adv. Atmos. Sci.*, **22**, 392–400.

Yuan, F., K. Wei, and W. Chen, 2010: Temporal variations of the frontal and monsoon storm rainfall during the first rainy season in South China. *Atmospheric and Oceanic Science Letters*, **3**, 243–247.

Yuan, Y., H. Yang, W. Zhou, and C. Y. Li, 2008: Influences of the Indian Ocean dipole on the Asian summer monsoon in the following year. *Int. J. Climatol.*, **28**, 1849–1859.

Zhang, Q. Y., and S. Y. Tao, 1998: Influence of Asian mid-high latitude circulation on East Asian summer rainfall. *Acta Meteorologica Sinica*, **56**, 199–211. (in Chinese).

Zhou, L. T., C. Y. Tam, W. Zhou, and J. C. L. Chan, 2010: Influence of South China Sea SST and the ENSO on winter rainfall over South China. *Adv. Atmos. Sci.*, **27**, 832–844.

Zhou, W., and J. C. L. Chan, 2005: Intraseasonal oscillations and the South China Sea summer monsoon onset. *Int. J. Climatol.*, **25**, 1585–1609.

Zhou, W., and J. C. L. Chan, 2007: ENSO and the South China Sea summer monsoon onset. *Int. J. Climatol.*, **27**, 157–167.

Zhou, W., J. C. L. Chan, and C. Y. Li, 2005: South China Sea summer monsoon onset in relation to the off-equatorial ITCZ. *Adv. Atmos. Sci.*, **22**, 665–676.

Zhou, W., C. Y. Li, and J. C. L. Chan, 2006: The interdecadal variations of the summer monsoon rainfall over South China. *Meteor. Atmos. Phys.*, **93**, 165–175.

Zhou, W., J. C. L. Chan, W. Chen, J. Ling, J. G. Pinto, and Y. P. Shao, 2009: Synoptic-scale controls of persistent low temperature and icy weather over Southern china in January 2008. *Mon. Wea. Rev.*, **137**, 3978–3991.